European Journal of Immunology

c-Jun N-terminal Kinase is a critical node in the death of $CD4^+CD8^+$ thymocytes during *Salmonella enterica* serovar Typhimurium infection

Mukta Deobagkar-Lele, Emmanuel S. Victor, Dipankar Nandi

Department of Biochemistry and Centre for Infectious Disease Research, Indian Institute of Science, Bangalore, INDIA

Keywords: cell death; glucocorticoids; interferon gamma; JNK activation; *Salmonella*; thymic atrophy

Corresponding author details:

Dipankar Nandi, Professor, Department of Biochemistry, FE14 Biological Sciences Building, Indian Institute of Science, Bangalore – 560012, India.

Email: nandi@biochem.iisc.ernet.in; Telephone No.: +91-8022933051; Fax No.: +91-8023600814

Received: March 7, 2013; Revised: August 15, 2013; Accepted: September 13, 2013

This article has been accepted for publication and undergone full peer review but has not been through the copyediting, typesetting, pagination and proofreading process, which may lead to differences between this version and the Version of Record. Please cite this article as an "Accepted Article", doi: 10.1002/eji.201343506.

Abstract

Thymic atrophy, due to the depletion of $CD4^+CD8^+$ thymocytes, is observed during infections with numerous pathogens. Several mechanisms, such as glucocorticoids and inflammatory cytokines are known to be involved in this process; however, the roles of intracellular signaling molecules have not been investigated. In this study, the functional role of c-Jun N-terminal kinase (JNK) during infection-induced thymic atrophy was addressed. The levels of phosphorylated JNK in immature $CD4^+CD8^+$ thymocytes from C57BL/6 (*Nramp*-deficient) and 129/SvJ (*Nramp*-sufficient) mice were increased upon oral infection of mice with *Salmonella enterica* serovar Typhimurium (*S. typhimurium*). Furthermore, inhibition of JNK signaling, but not ERK or p38 MAPK, prevented the in vitro death of infected thymocytes. Importantly, the in vivo inhibition of JNK signaling with SP600125 protected C57BL/6 $CD4^+CD8^+$ thymocytes from depletion via multiple mechanisms: lower intracellular ROS, inflammatory cytokines, Bax and caspase 3 activity, increase in Bcl-xL amounts and prevention of the loss in mitochondrial membrane potential. Notably, thymic architecture was preserved in infected mice treated with SP600125. Overall, this study identifies a novel role for JNK as a crucial regulator of the death of $CD4^+CD8^+$ thymocytes during *S. typhimurium* infection.

Introduction

The thymus plays a central role in the development of cell-mediated immunity and thymic atrophy resulting in loss of cellularity occurs during aging, stress and infections. Acute thymic atrophy is observed upon infection with viruses, bacteria, fungi, protists, etc [1]; however, the reasons and consequences of thymic atrophy are not well understood. Pathogens may elicit this response to reduce the cellular immune response; alternately, it may be a part of the host response to conserve energy and reduce the generation of T cells tolerant to the invading pathogen [2]. Indeed, T cells generated in thymi infected with *Mycobacterium avium* are tolerant to pathogen-specific antigens [3]. Infection with intracellular bacterial pathogens that multiply within host macrophages, such as *Francisella tularensis*, *Listeria monocytogenes*, and *Mycobacterium tuberculosis* leads to thymic atrophy [4-6]. Recent studies have shown that infection with attenuated [7] or virulent [8] Gram negative intracellular bacterium, *Salmonella enterica* serovar Typhimurium (*S. typhimurium*) also leads to thymic atrophy. *S. typhimurium* can breach the intestinal epithelial barrier in mice causing a systemic disease resembling typhoid caused by *S. typhi* in humans. Importantly, non-invasive *Salmonella* are known to establish an intracellular systemic disease in HIV-infected and immune-compromised individuals with a high degree of mortality and drug resistance [9,10]. Therefore, studies on all aspects of *Salmonella* pathogenesis are extremely important.

During infections, the thymus contracts and expands after clearance of the pathogen [11-12]. However, the consequences of thymic atrophy become more relevant during the development of peripheral lymphopenia due to infections (e.g. HIV) or chemotherapy. In fact, low thymic output is a major cause for failure of reconstitution of $CD4^+$ T-cell numbers in AIDS patients

undergoing anti-retroviral treatment [13-19]. Furthermore, the integrity of the adult thymus is required for other immune functions, e.g. affinity maturation of antibodies [20]. Therefore, it is important to understand the molecular and cellular processes involved during thymic atrophy as it may lead to the development of therapeutic targets. Several immune players are important during infection-induced thymic atrophy: glucocorticoids [5,6,8,21], inflammatory cytokines [5,6,8,21,22], reactive oxygen species (ROS) [23], activation of caspases [24], etc. Two recent studies have shown the cooperative roles of interferon gamma (IFN-γ) and glucocorticoids in mediating thymic atrophy during infection with virulent *Mycobacterium avium* [6] and *S. typhimurium* [8]. Despite numerous studies on the mechanisms involved during thymic atrophy, there is little information on the roles of intracellular signaling molecules involved in this process.

Mitogen activated protein kinases (MAPKs) are serine/threonine specific protein kinases with extracellular signal-regulated kinase (ERK), p38MAPK and c-Jun N-terminal kinase (JNK) being implicated in cell survival, stress responses [25,26]. MAPK pathways influence thymocyte development [27] and fetal thymic organ cultures show impaired negative, but not positive, selection with the inhibition of p38MAPK [28]. JNK activation leads to the downstream phosphorylation of c-Jun, which is important for the in vivo and in vitro depletion of $CD4^+CD8^+$ thymocytes via anti-CD3 [29,30]. The JNK1 signaling pathway plays a key role in T-cell responses [31] and thymocytes from *Jnk2*$^{-/-}$ mice are resistant to anti-CD3 mediated apoptosis [32]. In addition, thymocytes expressing the dominant negative JNK transgene are unable to undergo appropriate negative selection [33]. Although, JNK and other MAPKs are important in thymocyte death during development, there are no reports of their involvement during infection induced thymic atrophy.

The stress responsive kinase, JNK, is induced during several infections [34-37]. Upon infection of macrophages with *S. typhimurium*, JNK is upregulated via signal transduction pathways involving Herbimycin-sensitive tyrosine kinases, phosphoinositide 3-kinase and protein kinase zeta [37]. However, the functional roles of JNK during *S. typhimurium* infection are not known. Therefore, studies were performed to investigate the functional involvement of MAPKs during oral infection of mice with *S. typhimurium* leading to thymic atrophy [8]. Here we identify novel roles for JNK in the death of $CD4^+CD8^+$ thymocytes during *S. typhimurium* infection.

Results

JNK activation occurs primarily in immature thymocytes upon infection

To investigate the roles of signaling events during thymic atrophy, the total intracellular and phosphorylated amounts of JNK and p38MAPK were assessed in thymocytes 4 days after oral infection of C57BL/6 mice with *S. typhimurium*. Although total and phosphorylated p38MAPK were unaffected, intracellular JNK amounts were upregulated ~1.2 fold while pJNK amounts were upregulated ~2 fold in the total thymocyte population upon infection (Figure 1A-C). Upon gating of thymocyte subsets (Figure 1D), induction of pJNK was observed upon infection in $CD4^-CD8^-$ and $CD4^+CD8^+$ subsets (Figure 1E). Importantly, the increase in pJNK amounts was specific since it was absent in thymocytes from mice treated with SP600125 (Figure 1C, Figure 1E).

Ifnγ$^{-/-}$ mice treated with a single dose of 25 mg/kg of RU486, a glucocorticoid receptor antagonist, injected i.p. 12-16 h after oral infection are significantly protected from thymic atrophy upon *S. typhimurium* infection (Figure 1F). Also, compared with levels in infected

C57BL/6 mice, the pJNK amounts in the thymocytes from *Ifnγ*$^{-/-}$ mice were lower upon infection and RU486 treatment restored the elevated pJNK amounts to those of uninfected mice (Figure 1G). These data indicate that the infection induced glucocorticoid and IFN-γ-mediated pathways possibly lead to the downstream activation of JNK in thymocytes.

***S. typhimurium* infection-induced thymic atrophy also occurs in *Nramp*-sufficient mice**

C57BL/6 mice harbor a defective *Nramp* allele (*Nramp*-deficient), are highly susceptible to *S. typhimurium* infection with high CFU burden, display increased inflammatory cytokines, cortisol and extensive thymic atrophy [8]. However, the bacterial burden in humans, with the major population harboring a functional *NRAMP* allele, is much less [38]. To understand whether thymic atrophy and pJNK induction in thymocytes occur in *Nramp*-sufficient mice, 129/SvJ mice were infected with *S. typhimurium* orally. Consistent with a previous study [39], lower CFUs were recovered from 129/SvJ mice on days 5 and 15 post infection (Supporting Information Figure 1A, 1B). Although serum cortisol amounts remained unchanged, serum amounts of TNF-α, IFN-γ, IL-6 and IL-1β increased upon infection (Supporting Information Figure 1E, 1F, 1G, 1H) but were significantly reduced compared to those in C57BL/6 mice (Fig 6). However, a significant drop in $CD4^+CD8^+$ thymocyte numbers was observed upon infection with delayed kinetics (Supporting Information Figure 1D): day 5 in C57BL/6 compared to day 15 in 129/SvJ. Importantly, pJNK amounts in $CD4^+CD8^+$ thymocytes increased by day 15 (Supporting Information Figure 1F). Hence, thymic atrophy accompanied by elevated pJNK amounts is also observed upon infection with *S. typhimurium* in a *Nramp*-sufficient and a -resistant strain of mice.

JNK inhibition rescues in vitro death of infected thymocytes

To assess the functional relevance of JNK activation, thymocytes from control and infected C57BL/6 mice were cultured in vitro and viability was assessed. Viable cells from the infected group, but not the uninfected, were reduced significantly by 18 h in culture (Figure 2A) and the amounts of pJNK were elevated (Figure 2B). Inhibition of JNK by SP600125, but not ERK (PD98059) and p38MAPK (SB202190), rescued the in vitro death of thymocytes from infected mice (Figure 2C). Importantly, the rescue in cell viability was also accompanied by a concomitant decrease in pJNK, intracellular ROS, Annexin V positive cells and loss of mitochondrial membrane potential (Figure 2B, 2D-F).

Dexamethasone and IFN-γ–induced death of thymocytes is mediated via JNK

Since glucocorticoids and IFN-γ have been implicated in thymic atrophy during infection with virulent *Mycobacterium avium* [6] and *S. typhimurium* [8], the direct involvement of these molecules in thymocyte death and their relationship with JNK were investigated. Thymocytes from uninfected C57BL/6 mice underwent death in a dose-dependent manner when cultured in vitro in the presence of Dex, IFN-γ, ConA or anti-CD3 but not LPS or *S. typhimurium*. SP600125 rescued the Dex, IFN-γ and anti-CD3, but not ConA, mediated death in a dose dependent manner (Supporting Information Figure 2A-C). When a combination of Dex and IFN-γ were used at doses that individually did not affect thymocyte viability, $CD4^+CD8^+$ thymocytes, but not the other subsets, underwent death to a greater extent as compared to treatment with either signal alone (Figure 3A, 3B, Supporting Information Figure 2D). Importantly, the loss of viability was accompanied by a concomitant increase in pJNK, ROS and Annexin V and decrease in mitochondrial membrane potential which were rescued by SP600125 (Figure 3C-F, Supporting Information Figure 2E-G). Together these results indicate that JNK activation upon *S. typhimurium* infection is downstream to the glucocorticoid and IFN-γ-mediated pathways.

JNK activation is functionally important during the depletion of $CD4^+CD8^+$ thymocytes in vivo

The functional relevance of pJNK amounts, with respect to thymocyte survival during infection in vivo, was assessed. No significant differences were observed in the CFUs recovered from infected C57BL/6 mice upon SP600125 treatment (Figure 4A, 4B). Although the mesenteric lymph node (MLN) cell numbers decreased marginally, JNK inhibition had no effect on this ~1.5 fold depletion. Importantly, a dose dependent rescue in the ~ 8 fold drop in thymocyte numbers was observed with increasing doses of SP600125, wherein a single dose of 25 mg/kg and above delivered i.p. 12-16 hr after oral infection, rescued thymocyte death by ~80 % (Figure 4D). Also, SP600125 treatment did not have any adverse effects on the progression of infection and survival of mice (Figure 4E). Upon characterization of the thymocyte subsets during infection, a significant rescue was observed in the depletion of $CD4^+CD8^+$ thymocytes in the SP600125 treated mice as compared to the vehicle controls (Figure 4F). Importantly, the histological integrity of the thymus was maintained, with minimal damage to the typical thymic architecture, upon SP600125 treatment of infected mice. Both the cortex and medulla were structurally intact and the tissue sections from the SP600125 group closely resembled the control group (Figure 4G). Additionally, the infection-induced increase in ROS, Annexin V and caspase 3 activity and the decrease in mitochondrial potential in thymocytes were abrogated upon JNK inhibition (Figure 5A-D, Supporting Information Figure 3A, 3B).

To study the apoptotic process in further detail, the intracellular amounts of pro-apoptotic Bax and anti-apoptotic Bcl-xL, in thymocyte subsets upon infection, were studied. Importantly, the fold increase in Bax amounts upon infection was greater in $CD4^+CD8^+$

compared to single positive thymocytes and was lowered by SP600125 treatment (Figure 5E, Supporting Information Figure 3C). Concomitantly, the fold decrease in amounts of Bcl-xL was greater in $CD4^+CD8^+$ thymocytes upon infection compared to single positive thymocytes and was maintained by JNK inhibition (Figure 5F, Supporting Information Figure 3D).

JNK modulates the glucocorticoid and inflammatory cytokine pathways

As JNK inhibition has a profound protective effect on thymic atrophy, the JNK-mediated modulation of the glucocorticoid mediated signaling and inflammatory processes, were addressed with respect to thymic atrophy. Interestingly, administration of SP600125 lead to a small decrease in serum amounts of cortisol (Figure 6A). By day 4 post-infection, serum amounts of TNF-α, IFN-γ, IL-1β and IL-6 were significantly reduced upon SP600125 treatment compared to the vehicle treated groups (Figure 6B-E).

Discussion

During oral infection of C57BL/6 mice by *S. typhimurium* the numbers of immature $CD4^+CD8^+$ thymocytes, but not single positive and mature, $CD4^+$ and $CD8^+$ thymocytes or mesenteric lymph node cells, are greatly reduced [8]. In the present study, the functional roles of MAPKs during infection-induced thymic atrophy were investigated. Upon infection, the amounts of activated JNK, but not p38MAPK, were enhanced in C57BL/6 thymocytes (Figure 1). Also, the amounts of pJNK increased predominantly in the immature $CD4^-CD8^-$ and $CD4^+CD8^+$ thymocyte population and inhibition of JNK activation by SP600125 prevented this induction (Figure 1C, 1E). C57BL/6 mice are *Nramp*–deficient and are greatly susceptible to *S. typhimurium* infection with higher CFU burden and enhanced amounts of inflammatory cytokines [8, 39]. Since the CFU burden is low during *Salmonella* infection in

humans [38], a physiologically more relevant model was utilized. *Nramp*-sufficient 129/SvJ mice were infected with *S. typhimurium* orally and these mice had delayed infection kinetics with significantly low inflammatory cytokine amounts on day 5 and day 15 (Supporting Information Figure 1) [39]. However, there was a distinct drop in number of $CD4^+CD8^+$ thymocytes along with enhanced pJNK amounts by day 15 (Supporting Information Figure 1). Thus, *S. typhimurium* infection via the oral, i.e. the physiological, route leads to thymic atrophy in both, the *Nramp*-deficient C57BL/6 and the *Nramp*-sufficient 129/SvJ mice.

It is unlikely that direct interaction of *S. typhimurium* with thymocytes leads to their death during infection (Supporting Information Figure 2C). Most likely, the intracellular growth of bacteria within host cells leads to increase in the amounts of glucocorticoids, inflammatory cytokines, etc., which cooperate in enhancing the death of immature thymocytes [8]. Corticosteroids and IFN-γ are also produced within the thymus by the various cell types present therein [7, 40-42]. In this study, the direct in vitro effects of cortisol and IFN-γ in enhancing JNK activation, leading to the death of $CD4^+CD8^+$ thymocytes from C57BL/6 mice were addressed. Uninfected thymocytes were treated with Dex or IFN-γ which led to a dose dependent loss of cell viability (Supporting Information Figure 2A and B). A recent study has shown that the Dex-mediated transcriptional upregulation of the pro-apoptotic molecule, Bim, is via JNK [43]. Importantly, when a combination of Dex and IFN-γ was used, at doses that independently have less effect, significant $CD4^+CD8^+$ thymocyte death was observed. This was accompanied by increased pJNK, Annexin V and increased loss of mitochondrial membrane potential. Death under these conditions was rescued by the treatment of thymocytes with SP600125 (Figure 3), indicating that JNK activation is important during Dex and IFN-γ–mediated thymocyte death. Importantly, JNK activation in thymocytes upon infection was abrogated in mice lacking IFN-γ and treated with RU486

(Figure 1F). Together, these data reveal that glucocorticoids and IFN-γ are major regulators of JNK activation during infection-induced thymic atrophy in C57BL/6 (*Nramp*-deficient) mice.

The inhibition of JNK compromises the ability of some pathogens to infect host cells [35,36]. However, upon infection of C57BL/6 mice, organ CFUs (Figure 4B) and survival (Figure 4E) of infected mice were not affected by inhibition of JNK. Hence, any rescue observed in thymic atrophy would not be a consequence of reduced bacterial burdens during infection. This ensured that the JNK inhibitor, SP600125, could be used as a valid candidate to study the mechanisms involved during infection induced thymic atrophy. Strikingly, inhibition of JNK signaling abrogated the depletion of immature $CD4^+CD8^+$ thymocytes upon infection indicating that this is a critical signal during infection-induced thymic atrophy (Figure 4B, 4F). Most likely, this rescue is mediated via direct as well as indirect effects: First, studies with uninfected thymocytes demonstrated that the JNK inhibitor was able to "directly" block the glucocorticoid or IFN-γ-mediated death of immature thymocytes while lowering ROS and enhancing mitochondrial potential (Figure 3). Second, enhanced in vitro death of thymocytes from infected mice, compared to those from control mice, was observed. Most likely, thymocytes from infected mice were programmed to die quicker due to the signals perceived in vivo during infection (Figure 2A). Also, inhibition of JNK, but not ERK or p38MAPK, rescued the survival of thymocytes, which correlated with lower Annexin V, ROS and normal mitochondrial membrane potential (Figure 2C-F). Extensive mitochondrial damage during apoptosis is associated with the activation of JNK, and its interactions with mitochondrial pro-apoptotic proteins [44,45]. JNK not only regulates mitochondria-mediated apoptosis but also increases the phosphorylation of c-Jun in AP-1. Inhibition of JNK leads to lack of Bcl2 phosphorylation and protects hepatocytes from acetaminophen-induced death [46].

Additionally, in a carcinoma cell line, the JNK-specific inhibitor abolished mevastatin-induced cell growth inhibition and apoptosis [47]. Also, thymocytes have a distinct distribution of pro and anti-apoptotic proteins and they are exquisitely sensitive to the action of Bcl2 family proteins [48]. Finally, upon inhibition of JNK signaling during in vivo infection, significant rescue in $CD4^+CD8^+$ thymocyte numbers were observed (Figure 4D). Also, there were lower amounts of ROS, mitochondrial damage and caspase 3 activity. In addition, the fold increase in Bax and decease in Bcl-xL amounts in $CD4^+CD8^+$ thymocytes was rescued by JNK inhibition (Figures 4E, 4F, 5 and Supporting Information Figure 3). Together, these data suggest that JNK activation directly leads to cell death.

In addition, there are probably indirect mechanisms by which the JNK inhibitor blocks death of $CD4^+CD8^+$ thymocytes during infection. Thymic architecture, which is known to be disorganized during some models of thymic atrophy [5,6,8,21,22], was well preserved upon SP600125 administration during infection (Figure 4G). It is possible that the SP600125-mediated protection of thymocytes from in vivo death signals during infection may be a consequence of the maintenance of thymic environment, which is critical during thymocyte development. Additionally, JNK has been implicated in the development of insulin resistance, neurological and cardiac disorders as well as many inflammatory diseases, including rheumatoid arthritis [49]. The JNK inhibitor lowered the amounts of cortisol in a modest manner during infection; however, it significantly reduced the amounts of inflammatory cytokines (Figure 6). Further studies are required to correlate the amounts of organ-specific cytokines with bacterial burden. Also, the types of cells producing these cytokines and their regulation during infection need to be pursued. It may be worthwhile to remember these caveats while correlating the effects of inflammatory cytokines during thymic atrophy.

Studies using RU486 and *Ifnγ*$^{-/-}$ mice revealed the roles of glucocorticoids and IFN-γ in enhancing JNK activation (Figure 1G). It is possible that some feed back regulatory processes exist that enhanced the amounts of cortisol and inflammatory cytokines upon JNK activation (Figure 6). Most likely, the high efficiency of the JNK inhibitor in reducing thymic atrophy was due to its ability to work at multiple stages: direct (Figure 2 and Figure 3), indirect (Figure 4 and Figure 5) and effects on thymic architecture (Figure 4G). Further studies using genetic knockout mice are necessary to delineate the specific contributions of its isoforms JNK1, JNK2 and JNK3 during infection induced thymic atrophy. In this study, SP600125 was used which inhibits all the isoforms of JNK. Also, the roles of other MAPK pathway components and the downstream signaling molecules that might interact with these leading to thymocyte death need to be deciphered.

During prolonged chronic infections or chemotherapy, thymic atrophy is observed together with peripheral lymphopenia. Under these circumstances, thymic atrophy may lead to the generation of lower numbers of mature T cells and hamper the host's ability to respond to immune challenges. In this model, a small degree of peripheral lymphopenia accompanies the massive thymic atrophy; however this appears to be independent of cortisol, IFN-γ [8] and JNK activation (Figure 4C). The present model of study is an acute and lethal infection model, wherein mice die by 10-15 days. Therefore, it is difficult to comment upon the consequences of the observed lymphopenia and thymic atrophy in host resistance to subsequent immune challenges. However, HIV-infected individuals with extensive peripheral lymphopenia also exhibit enhanced thymic atrophy and reduced thymic output. Interestingly, anti-retroviral therapy not only supports peripheral $CD4^+$ T-cell reconstitution but also boosts thymic function, indicating that the thymus may play a role in immune reconstitution [13-19].

Thus, understanding the mechanisms involved in thymic atrophy may influence therapeutic regimes where thymic output may be an important parameter. Consequently, the combination of anti-microbial compounds and compounds that boost thymic function may prove to be extremely beneficial. As shown in this study, the high efficacy of the inhibition of JNK activation in rescuing infection-induced thymic atrophy makes this molecule a good target for such strategies. Further studies will be required to evaluate the role of JNK activation during other models of thymic atrophy.

JNK plays an important role during thymocyte development [29-33]; consequently, long term JNK inhibition may increase the number of self reactive T cells that may result in autoimmunity. This aspect needs careful consideration; however, several small molecule JNK inhibitors are under development as anti-inflammatory molecules during arthritis and Crohn's disease [49-53]. To the best of our knowledge, this study is the first to demonstrate a role of JNK activation during infection-induced thymic atrophy. Further studies will be required to evaluate the roles of JNK inhibitors during thymic atrophy caused by other pathogens and their clinical relevance.

Materials and methods

Bacterial cultures and inhibitors. *S. typhimurium* NCTC 12023 was used for oral infection of mice [54]. Bacteria were cultured overnight in Luria broth from a single colony on a salmonella-shigella agar plate. The overnight pre-inoculum was used at 0.2 % in fresh 50 ml Luria broth to obtain a log phase culture (3-4 hr, 160 rpm, 37°C) and bacteria were resuspended in sterile PBS. RU486 (Mifepristone, a progesterone and glucocorticoid receptor antagonist) and SP600125 or JNK Inhibitor II (a reversible, ATP-competitive inhibitor for JNK1, 2 and 3) [55] were purchased from Sigma Aldrich Ltd., USA, dissolved in DMSO and injected i.p. at the indicated doses. Inhibitors were administered once i.p. 12-16 h after oral infection. PD98059 (a selective MEK1-ERK1 inhibitor) and SB202190 (a highly potent and cell permeable inhibitor of p38MAPKs) were purchased from Calbiochem, USA, and dissolved in DMSO. Lipopolysaccharide (LPS), dexamethasone (Dex, a synthetic glucocorticoid) and concanavalin A (ConA) were purchased from Sigma Aldrich Ltd., USA. Recombinant mouse IFNγ was purchased from PeproTech, Israel.

Mice and infection protocol. 6-8 week-old C57BL/6 and C57BL/6.*Ifnγ*$^{-/-}$ (*Ifnγ*$^{-/-}$) mice were bred and maintained at the Central Animal Facility of IISc. 129/SvJ mice were obtained from Jawaharlal Nehru Centre for Advanced Scientific Research, Bangalore and maintained at the Central Animal Facility of IISc. Mice were given an oral dose of ~10^8 - 10^9 CFU *S. typhimurium* in a total volume of 0.5 ml PBS. Each experimental group had between 3 to 12 mice. All experiments were performed upon approval and in accordance with the guidelines stated by the Institutional Animal Ethics Committee, IISc. On indicated days post infection, mice were sacrificed and the CFU load in tissue samples was enumerated by plating tissue homogenates on salmonella-shigella agar. Blood collected upon sacrificing the mice was

allowed to clot and centrifuged, and serum was stored at -20°C for further analysis. The survival of mice was monitored at 12 h intervals for a period of 15 days post infection.

Cytokines and cortisol measurement. Serum amounts of TNF-α, IFN-γ, IL-1β and IL-6 were measured using ELISA kits (eBioscience, USA) and cortisol amounts were measured by an AccuBind ELISA kit (Monobind, Inc., USA) according to manufacturers' instructions.

Isolation and culture of lymph node cells and thymocytes. On indicated days post infection, mice were sacrificed and MLN and thymi were dissected. The tissues were washed in PBS, weighed and disrupted using forceps and fine wire mesh to prepare single cell suspensions in RPMI + 5 % FCS [56]. Viable cell numbers were determined using Trypan blue staining and counting was done with a haemocytometer. Thymocytes from control and infected mice were cultured in 96 well round bottom plates at a density of 0.3 million cells per well with or without inhibitors and viable cells were estimated at indicated time points.

Flow cytometric analysis. Cell surface markers and intracellular signaling analysis was performed on a BD Canto II flow analyzer. FITC- or allophycocyanin-conjugated monoclonal antibodies against CD4 and PE-conjugated antibodies against CD8 were obtained from eBioscience, USA. Rabbit polyclonal antibodies against total and phosphorylated JNK and total p38MAPK were obtained from Millipore USA. Anti-phospho p38MAPK was obtained from Imgenex, USA and FITC-conjugated anti-rabbit and anti-mouse monoclonal antibodies were from Jackson ImmunoResearch, USA. Anti-mouse Bcl-xL and Bax antibodies were obtained from Cell Signaling Technology, USA. Briefly, cells were incubated with fluorophore tagged antibodies against surface markers, washed, fixed and resuspended in small volumes of permeabilization buffer. Cells were incubated with specific

antibodies against intracellular proteins which were detected using appropriate secondary antibodies. The stained samples were resuspended in 0.5 % paraformaldehyde before acquiring FACS data. Live cell populations were gated on the basis of forward and side scatter. Thymocyte subsets were gated on the basis of CD4 and CD8 expression (Figure 1D). All FACS data were analyzed using the BD Diva and WinMDI softwares.

Cell death and mitochondrial assays. Cell death was assayed using FITC-conjugated AnnexinV and Propidium iodide (PI) from BD Biosciences, USA. Briefly, thymocytes were incubated with AnnexinV-FITC in binding buffer for 30 min on ice followed by washing and PI addition before data was acquired on a BD Canto II. Caspase 3 activity colorimetric assay was performed according to manufacturer's instructions using a kit from Sigma Aldrich Ltd., USA. Changes in mitochondrial membrane potential were analyzed by incubating cells with 100 nM MitoTracker Red CMXROS (Invitrogen, USA) at 37°C for 30 min, washing cells and acquiring data on a BD Canto II. Cells with damaged mitochondria had lesser accumulation of MitoTracker Red CMXROS and these populations were quantified. Similarly, intracellular reactive oxygen species (ROS) were measured by incubating cells with 10 μM 5-(and-6)-Carboxy-2',7'-Dichlorofluorescein Diacetate (DCFDA) for 15 min at 37°C , washing off excess dye and acquiring data on the flow cytometer.

Histological examination. MLN and thymi were dissected, washed in PBS and fixed in 10 % neutral buffered formalin. The tissues were embedded in paraffin wax and the sections were stained with haematoxylin and eosin (H & E). Slides were observed under an inverted light microscope and 100X magnified images were acquired on a Nikon camera attached to the microscope.

Statistical analysis. Data were plotted and analyzed using commercially available software (WinMDI, Microsoft Excel and GraphPad Prism 5). The quantified data from independent experiments are presented as mean +/- SEM. Statistically significant differences between various parameters were assessed by means of Student's *t* test with 95% confidence interval and *p* values were reported as follows * $p<0.05$, ** $p<0.01$, *** $p<0.001$.

Acknowledgements

The authors thank the Central Animal Facility, IISc and JNCASR, Bangalore for the supply of mice for these experiments. All personnel at the Flow Cytometry Divisional Facility, IISc, are gratefully acknowledged for their patience and timely help. The authors deeply appreciate the support and encouragement of all members of the DpN laboratory. This work was supported by grants from the Department of Biotechnology (DBT), India. MDL received SPM fellowship from Council of Scientific and Industrial Research (CSIR), India.

Conflict of interest statement: The authors declare no financial or commercial conflict of interest.

References

1. **Savino, W.,** The thymus is a common target organ in infectious diseases. *PLoS Pathog.* 2006. **2**: e62.
2. **Dooley, J. and Liston, A.,** Molecular control over thymic involution: from cytokines and microRNA to aging and adipose tissue. *Eur. J. Immunol.* 2012. **42**: 1073-9.
3. **Nobrega, C., Roque, S., Nunes-Alves, C., Coelho, A., Medeiros, I., Castro, A. G., Appelberg, R. and Correia-Neves, M.,** Dissemination of mycobacteria to the thymus renders newly generated T cells tolerant to the invading pathogen. *J. Immunol.* 2010. **184**: 351-8.
4. **Mandel, T. E. and Cheers, C.,** Resistance and susceptibility of mice to bacterial infection: histopathology of listeriosis in resistant and susceptible strains. *Infect. Immun.* 1980. **30**: 851-61.
5. **Chen, W., Kuolee, R., Austin, J. W., Shen, H., Che, Y. and Conlan, J. W.,** Low dose aerosol infection of mice with virulent type A *Francisella tularensis* induces severe thymus atrophy and $CD4^+CD8^+$ thymocyte depletion. *Microb. Pathog.* 2005. **39**: 189-96.
6. **Borges, M., Barreira-Silva, P., Flórido, M., Jordan, M. B., Correia-Neves, M., and Appelberg, R.,** Molecular and cellular mechanisms of *Mycobacterium avium*-induced thymic atrophy. *J. Immunol.* 2012. **189**: 3600-8.
7. **Ross, E. A., Coughlan, R. E., Flores-Langarica, A., Lax, S., Nicholson, J., Desanti, G. E., Marshall, J. L. *et al.*** Thymic function is maintained during Salmonella-induced atrophy and recovery. *J. Immunol.* 2012. **189**: 4266-74.
8. **Deobagkar-Lele, M., Chacko, S. K., Victor, E. S., Kadthur, J. C. and Nandi, D.,** Interferon γ and Glucocorticoid Mediated Pathways Synergize to Enhance Death of

CD4(+) CD8(+) Thymocytes during *Salmonella enterica* serovar Typhimurium Infection. *Immunology*. 2012. DOI: 10.1111/imm.12047.

9. **Crump, J. A. and Mintz, E. D.,** Global trends in typhoid and paratyphoid Fever. *Clin. Infect. Dis.* 2010. **50**: 241-6.
10. **Gordon, M. A., Kankwatira, A. M., Mwafulirwa, G., Walsh, A. L., Hopkins, M. J., Parry, C. M., Faragher, E. B. *et al.*,** Invasive non-typhoid salmonellae establish systemic intracellular infection in HIV-infected adults: an emerging disease pathogenesis. *Clin. Infect. Dis.* 2010. **50**: 953-62.
11. **Godfraind, C., Holmes, K. V. and Coutelier, J. P.,** Thymus involution induced by mouse hepatitis virus A59 in BALB/c mice. *J. Virol.* 1995. **69**: 6541-7.
12. **Rosenzweig, M., Connole, M., Forand-Barabasz, A., Tremblay, M. P., Johnson, R. P. and Lackner, A. A.,** Mechanisms associated with thymocyte apoptosis induced by simian immunodeficiency virus. *J. Immunol.* 2000. **165**: 3461-8.
13. **Dion, M. L., Poulin, J. F., Bordi, R., Sylvestre, M., Corsini, R., Kettaf, N., Dalloul, A. *et al.*,** HIV infection rapidly induces and maintains a substantial suppression of thymocyte proliferation. *Immunity*. 2004. **21**: 757-68.
14. **Ho Tsong Fang, R., Colantonio, A. D. and Uittenbogaart, C. H.,** The role of the thymus in HIV infection: a 10 year perspective. *AIDS*. 2008. **22**: 171-184.
15. **van den Brink, M. R., Alpdogan, O. and Boyd, R. L.,** Strategies to enhance T-cell reconstitution in immuno-compromised patients. *Nat. Rev. Immunol.* 2004. **4**: 856-867.
16. **Lee, J. C., Boechat, M. I., Belzer, M., Church, J. A., De Ville, J., Nielsen, K., Weston, S. *et al.*,** Thymic volume, T-cell populations, and parameters of thymopoiesis in adolescent and adult survivors of HIV infection acquired in infancy. *AIDS*. 2006. **20**: 667-674.

17. **Westrop, S. J., Qazi, N. A., Pido-Lopez, J., Nelson, M. R., Gazzard, B., Gotch, F. M. and Imami, N.,** Transient nature of long-term nonprogression and broad virus-specific proliferative T-cell responses with sustained thymic output in HIV-1 controllers. *PLoS One.* 2009. **4**: e5474

18. **Li, T., Wu, N., Dai, Y., Qiu, Z., Han, Y., Xie, J., Zhu, T. and Li, Y.,** Reduced thymic output is a major mechanism of immune reconstitution failure in HIV-infected patients after long-term antiretroviral therapy. *Clin. Infect. Dis.* 2011. **53**: 944-51.

19. **Garrido, C., Rallón, N., Soriano, V., Lopez, M., Zahonero, N., de Mendoza, C. and Benito, J. M.,** Mechanisms involved in CD4 cell gains in HIV-infected patients switched to raltegravir. *AIDS.* 2012. **26**: 551-7.

20. **AbuAttieh, M., Bender, D., Liu, E., Wettstein, P., Platt, J. L. and Cascalho, M.**, Affinity maturation of antibodies requires integrity of the adult thymus. *Eur. J. Immunol*. 2012. **42**: 500-10.

21. **Pérez, A. R., Roggero, E., Nicora, A., Palazzi, J., Besedovsky, H. O., Del Rey, A. and Bottasso, O. A.,** Thymus atrophy during *Trypanosoma cruzi* infection is caused by an immuno-endocrine imbalance. *Brain Behavior Immunity* 2007. **21**: 890-900.

22. **Billard, M. J., Gruver, A. L. and Sempowski, G. D.,** Acute endotoxin-induced thymic atrophy is characterized by intrathymic inflammatory and wound healing responses. *PLoS One*. 2011. **6**: e17940.

23. **Scofield, V. L., Yan, M., Kuang, X., Kim, S. J. and Wong, P. K.,** The drug monosodium luminol (GVT) preserves crypt-villus epithelial organization and allows survival of intestinal T cells in mice infected with the ts1 retrovirus. *Immunol. Lett.* 2009. **122**: 150-8.

24. **Farias-de-Oliveira, D. A., Villa-Verde, D. M., Nunes Panzenhagen, P. H., Silva Dos Santos, D., Berbert, L. R., Savino, W. and de Meis, J.,** Caspase-8 and caspase-9

mediate thymocyte apoptosis in *Trypanosoma cruzi* acutely infected mice. *J. Leukoc. Biol.* 2013. **93**: 227-34

25. **Seger, R. and Krebs, E. G.,** The MAPK signaling cascade. *FASEB. J.* 1995. **9**: 726-35.
26. **Johnson, G. L. and Lapadat, R.,** Mitogen-activated protein kinase pathways mediated by ERK, JNK, and p38 protein kinases. *Science*. 2002. **298**: 1911-2
27. **Werlen, G., Hausmann, B., Naeher, D. and Palmer, E.,** Signaling life and death in the thymus: timing is everything. *Science.* 2003. **299**: 1859-63.
28. **Sugawara, T., Moriguchi, T., Nishida, E. and Takahama, Y.,** Differential roles of ERK and p38 MAP kinase pathways in positive and negative selection of T lymphocytes. *Immunity.* 1998 **9**: 565-74.
29. **Rincón, M., Whitmarsh, A., Yang, D. D., Weiss, L., Dérijard, B., Jayaraj, P., Davis, R. J. and Flavell RA.,** The JNK pathway regulates the in vivo deletion of immature $CD4^+CD8^+$ thymocytes. *J. Exp. Med.* 1998. **188**: 1817-1830
30. **Behrens, A., Sabapathy, K., Graef, I., Cleary, M., Crabtree, G. R. and Wagner, E. F.,** Jun N-terminal kinase 2 modulates thymocyte apoptosis and T cell activation through c-Jun and nuclear factor of activated T cell (NF-AT). *Proc. Natl. Acad. Sci.* USA. 2001. **98**: 1769-74.
31. **Dong, C., Yang, D. D., Wysk, M., Whitmarsh, A. J., Davis, R. J. and Flavell, R. A.,** Defective T cell differentiation in the absence of Jnk1. *Science*. 1998. **282**: 2092-5.
32. **Sabapathy, K., Hu, Y., Kallunki, T., Schreiber, M., David, J. P., Jochum, W., Wagner, E. F. and Karin, M.,** JNK2 is required for efficient T-cell activation and apoptosis but not for normal lymphocyte development. *Curr. Biol.* 1999. **9**: 116-25.
33. **Sabapathy, K., Kallunki, T., David, J. P., Graef, I., Karin, M. and Wagner, E. F.,** c-Jun NH2-terminal kinase (JNK)1 and JNK2 have similar and stage-dependent roles in regulating T cell apoptosis and proliferation. *J. Exp. Med.* 2001. **193**:317-28.

34. **Clarke, P., Meintzer, S. M., Widmann, C., Johnson, G. L. and Tyler, K. L.,** Reovirus infection activates JNK and the JNK-dependent transcription factor c-Jun. *J. Virol.* 2001. **75**: 11275-83

35. **Manganaro, L., Lusic, M., Gutierrez, M. I., Cereseto, A., Del Sal, G. and Giacca, M.,** Concerted action of cellular JNK and Pin1 restricts HIV-1 genome integration to activated $CD4^+$ T lymphocytes. *Nat. Med.* 2010. **16**: 329-33.

36. **Ceballos-Olvera, I., Chávez-Salinas, S., Medina, F., Ludert, J. E and del Angel, R. M.,** JNK phosphorylation, induced during dengue virus infection, is important for viral infection and requires the presence of cholesterol. *Virology*. 2010. **396**: 30-6.

37. **Procyk, K. J., Rippo, M. R., Testi, R., Hoffmann, F., Parker, P. J. and Baccarini M.,** Distinct mechanisms target stress and extracellular signal-activated kinase 1 and Jun N-terminal kinase during infection of macrophages with *Salmonella*. *J. Immunol.* 1999. **163**: 4924-30.

38. **Wain, J., Diep, T. S., Ho, V. A., Walsh, A. M., Nguyen, T. T., Parry, C. M., and White, N. J.,** Quantitation of bacteria in blood of typhoid fever patients and relationship between counts and clinical features, transmissibility, and antibiotic resistance. *J. Clin. Microbiol.* 1998. **36**:1683-7.

39. **Monack, D. M., Bouley, D. M. and Falkow, S.,** *Salmonella typhimurium* persists within macrophages in the mesenteric lymph nodes of chronically infected *Nramp1*$^{+/+}$ mice and can be reactivated by IFNgamma neutralization. *J. Exp. Med.* 2004. **199**:231-41.

40. **Ashwell, J. D., Lu, F. W. and Vacchio, M. S.,** Glucocorticoids in T cell development and function. *Annu. Rev. Immunol.* 2000. **18**:309-45.

41. **Liang, Y., Hudson, L. C., Levy, J. K., Ritchey, J. W., Tompkins, W. A. and Tompkins, M. B.,** T cells overexpressing interferon-gamma and interleukin-10 are

found in both the thymus and secondary lymphoid tissues of feline immunodeficiency virus-infected cats. *J. Infect. Dis.* 2000. **181**:564-75.

42. **Boehm, U., Klamp, T., Groot, M. and Howard, J. C.,** Cellular responses to interferon-gamma. *Annu. Rev. Immunol.* 1997. **15**:749-95.
43. **Heidari, N., Miller, A. V., Hicks, M. A., Marking, C. B. and Harada, H.,** Glucocorticoid-mediated BIM induction and apoptosis are regulated by Runx2 and c-Jun in leukemia cells. *Cell. Death. Dis.* 2012. **3**: e349.
44. **Kharbanda, S., Saxena, S., Yoshida, K., Pandey, P., Kaneki, M., Wang, Q., Cheng, K. et al.,** Translocation of SAPK/JNK to mitochondria and interaction with Bcl-xL in response to DNA damage. *J. Biol. Chem.* 2000. **275**: 322-7.
45. **Dhanasekaran, D. N. and Reddy, E. P.,** JNK signaling in apoptosis. *Oncogene*. 2008. **27**: 6245-51.
46. **Latchoumycandane, C., Seah, Q. M., Tan, R. C., Sattabongkot, J., Beerheide, W. and Boelsterli, U. A.,** Leflunomide or A77 1726 protect from acetaminophen-induced cell injury through inhibition of JNK-mediated mitochondrial permeability transition in immortalized human hepatocytes. *Toxicol. Appl. Pharmacol.* 2006. **217**: 125-33.
47. **Zhang, S., Wang, X. L., Gan, Y. H. and Li, S. L.,** Activation of c-Jun N-terminal kinase is required for mevastatin-induced apoptosis of salivary adenoid cystic carcinoma cells. *Anticancer Drugs*. 2010. **21**: 678-86.
48. **Chao, D. T. and Korsmeyer, S. J.,** BCL-2 family: regulators of cell death. *Annu. Rev. Immunol.* 1998. **16**:395-419.
49. **Hammaker, D. R., Boyle, D. L., Chabaud-Riou, M. and Firestein, G. S.,** Regulation of c-Jun N-terminal kinase by MEKK-2 and mitogen-activated protein kinase kinase kinases in rheumatoid arthritis. *J. Immunol*. 2004. **172**: 1612-8.

50. **Han, Z., Boyle, D. L., Chang, L., Bennett, B., Karin, M., Yang, L., Manning, A. M. and Firestein, G. S.,** c-Jun N-terminal kinase is required for metalloproteinase expression and joint destruction in inflammatory arthritis. *J. Clin. Invest.* 2001. **108**: 73– 81.

51. **Hommes, D., van den Blink, B., Plasse, T., Bartelsman, J., Xu, C., Macpherson, B., Tytgat, G. *et al.*,** Inhibition of stress-activated MAP kinases induces clinical improvement in moderate to severe Crohn's disease. *Gastroenterology.* 2002. **122**: 7–14.

52. **Manning, A. M. and Davis, R. J.,** Targeting JNK for therapeutic benefit: from junk to gold? *Nat. Rev. Drug. Discov.* 2003. **2**: 554-565.

53. **Bogoyevitch, M. A., Boehm, I., Oakley, A., Ketterman, A. J. and Barr, R. K.,** Targeting the JNK MAPK cascade for inhibition: basic science and therapeutic potential. *Biochim. Biophys. Acta.* 2004. **1697**: 89-101.

54. **Bhosale, M., Kadthur, J. C. and Nandi, D.,** Roles of *Salmonella enterica* serovar Typhimurium encoded Peptidase N during systemic infection of *Ifnγ*$^{-/-}$ mice. *Immunobiology*. 2012. **217**: 354-62.

55. **Bennett, B. L., Sasaki, D. T., Murray, B. W., O'Leary, E. C., Sakata, S. T., Xu, W., Leisten, J. C., *et al.*,** SP600125, an anthrapyrazolone inhibitor of Jun N-terminal kinase. *Proc. Natl. Acad. Sci. USA.* 2001. **98**: 13681-6.

56. **Patil, V., Kumar, A., Kuruppath, S. and Nandi, D.,** Peptidase N encoded by *Salmonella enterica* serovar Typhimurium modulates systemic infection in mice. *FEMS. Immunol. Med. Microbiol.* 2007. **51**: 431-42.

Figure 1. Intracellular pJNK increases in $CD4^+CD8^+$ thymocytes upon *S. typhimurium* infection. C57BL/6 mice were orally infected with 10^8 CFUs of *S. typhimurium* and treated with either SP600125 (25 mg/kg) or RU486 (25 mg/kg). On day 4 post infection, uninfected and infected mice were sacrificed and intracellular amounts of (A) p38MAPK and p-p38MAPK and (B) JNK and pJNK were estimated by flow cytometry. (C) Representative flow cytometry plots of JNK and pJNK amounts in total thymocytes from uninfected (UI), infected (*Stm*) and infected with SP600125 treated (*Stm* + SP600125) mice are shown. (D) The gating strategy for analysis of pJNK expression in $CD4^-CD8^-$, $CD4^+CD8^+$, $CD4^+CD8^-$ and $CD4^-CD8^+$ thymocytes upon infection, with and without SP600125 treatment are depicted. (E) Representative flow cytometry plots (left) and quantification of pJNK expression in the indicated thymocyte subsets (right) are shown. (F) Viable cell number and (G) pJNK amounts in thymocytes upon treatment of infected C57BL/6 and *Ifnγ*$^{-/-}$ mice with RU486 is shown. (A, B, E-G) Data are shown as mean + SEM of 3-5 mice per group from one experiment representative of three independent experiments. $p \leq 0.05$, ** $p \leq 0.01$ and *** $p \leq 0.001$, Student's *t* test.

Figure 1

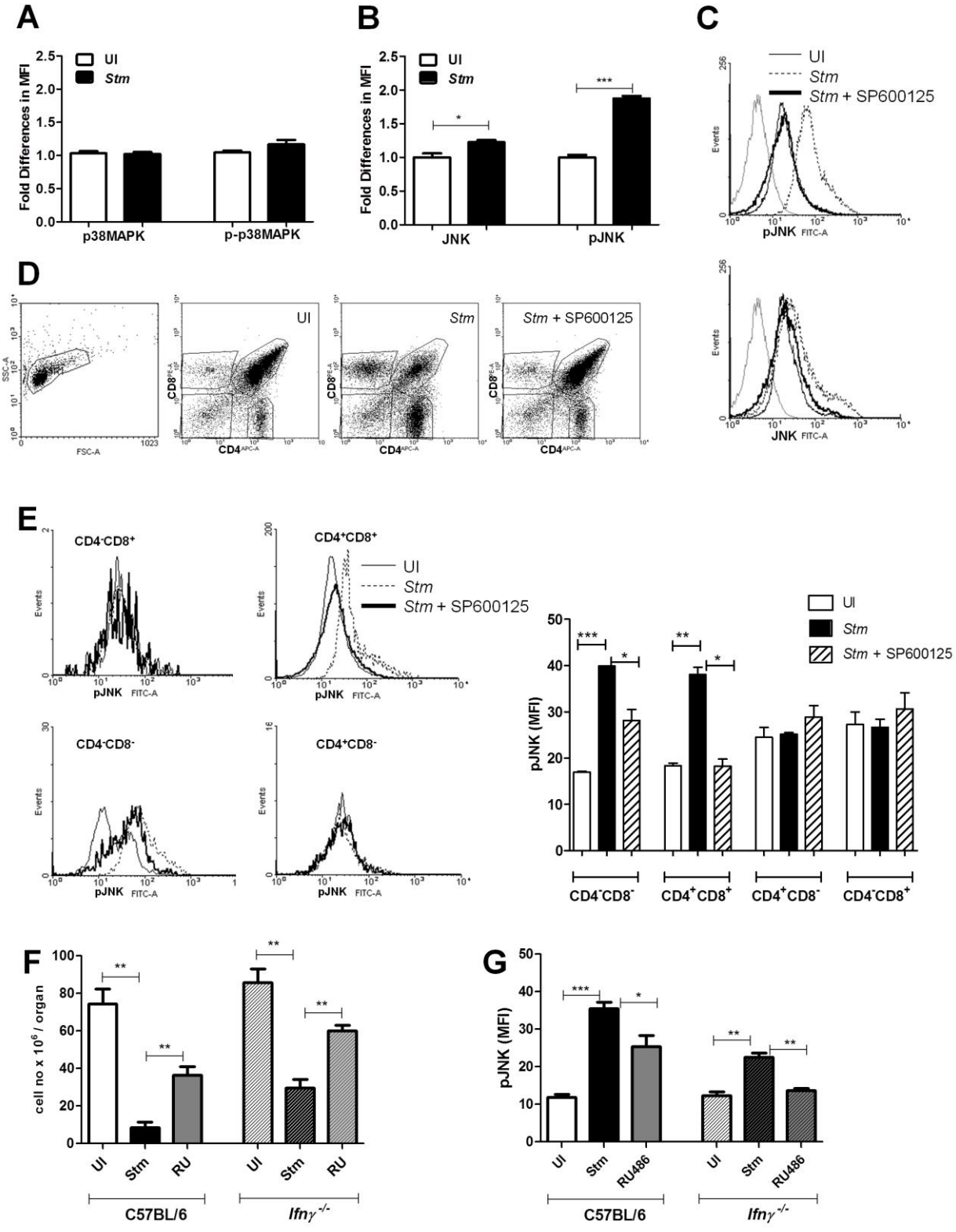

Figure 2. Inhibition of JNK signaling rescues in vitro death of thymocytes from infected mice. C57BL/6 mice were orally infected with 10^8 CFU *S. typhimurium*. (A) On day 4 post infection the in vitro survival of thymocytes from uninfected (UI) and infected (*Stm*) mice was assessed at different time points. (B) Intracellular amounts of pJNK in CT and ST upon SP600125 treatment were estimated by flow cytometry and a representative histogram is depicted (right). (C) Viable cell numbers of UI and *Stm* upon treatment with indicated doses of SP600125, PD98059 and SB202190 for 18 h were measured by Trypan blue exclusion. (D-F) Thymocytes from uninfected and infected mice were treated with SP600125 for 18 h and (D) intracellular ROS, (E) extent of apoptosis by Annexin V and (F) loss of mitochondrial potential were measured by flow cytometry. The data are shown as mean + SEM of three experiments in which cells from 2-3 mice were pooled per experiment. * $p \leq 0.05$, ** $p \leq 0.01$ and *** $p \leq 0.001$, Student's *t* test.

Figure 2

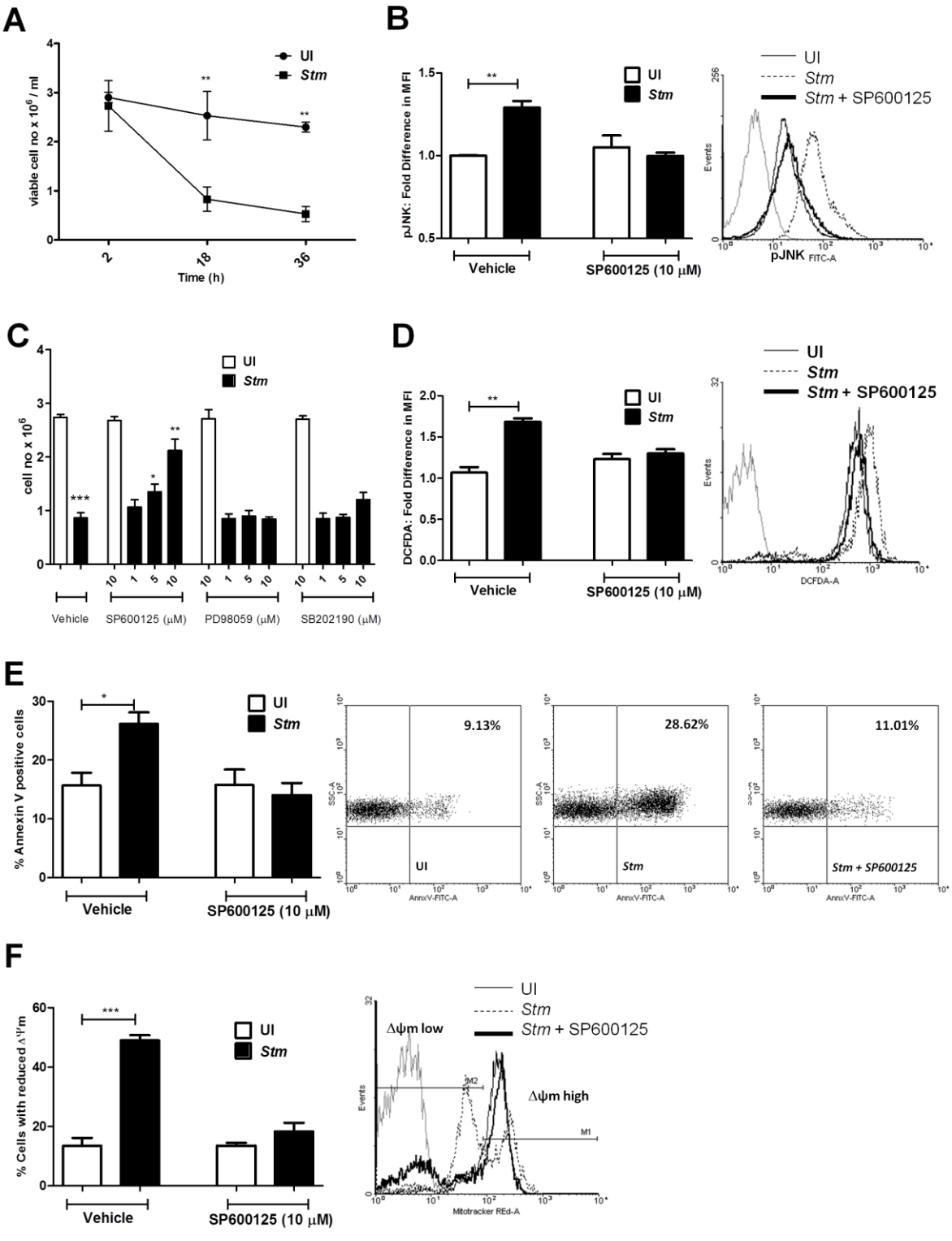

Figure 3. IFN-γ and glucocorticoids together lead to activation of JNK and apoptosis of $CD4^+CD8^+$ thymocytes. Thymocytes from uninfected C57BL/6 mice were isolated and cultured in vitro with indicated doses of Dex in combination with IFN-γ in the presence and absence of SP600125. (A) viable cell numbers, (B) percentage of $CD4^+CD8^+$ thymocytes, (C) intracellular pJNK amounts, (D) extent of apoptosis, (E) intracellular ROS and (F) loss of mitochondrial potential were measured. The data are shown as mean + SEM of two independent experiments in which cells from 3 mice were pooled per experiment. * $p \leq 0.05$, ** $p \leq 0.01$ and *** $p \leq 0.001$, Student's *t* test.

Figure 3

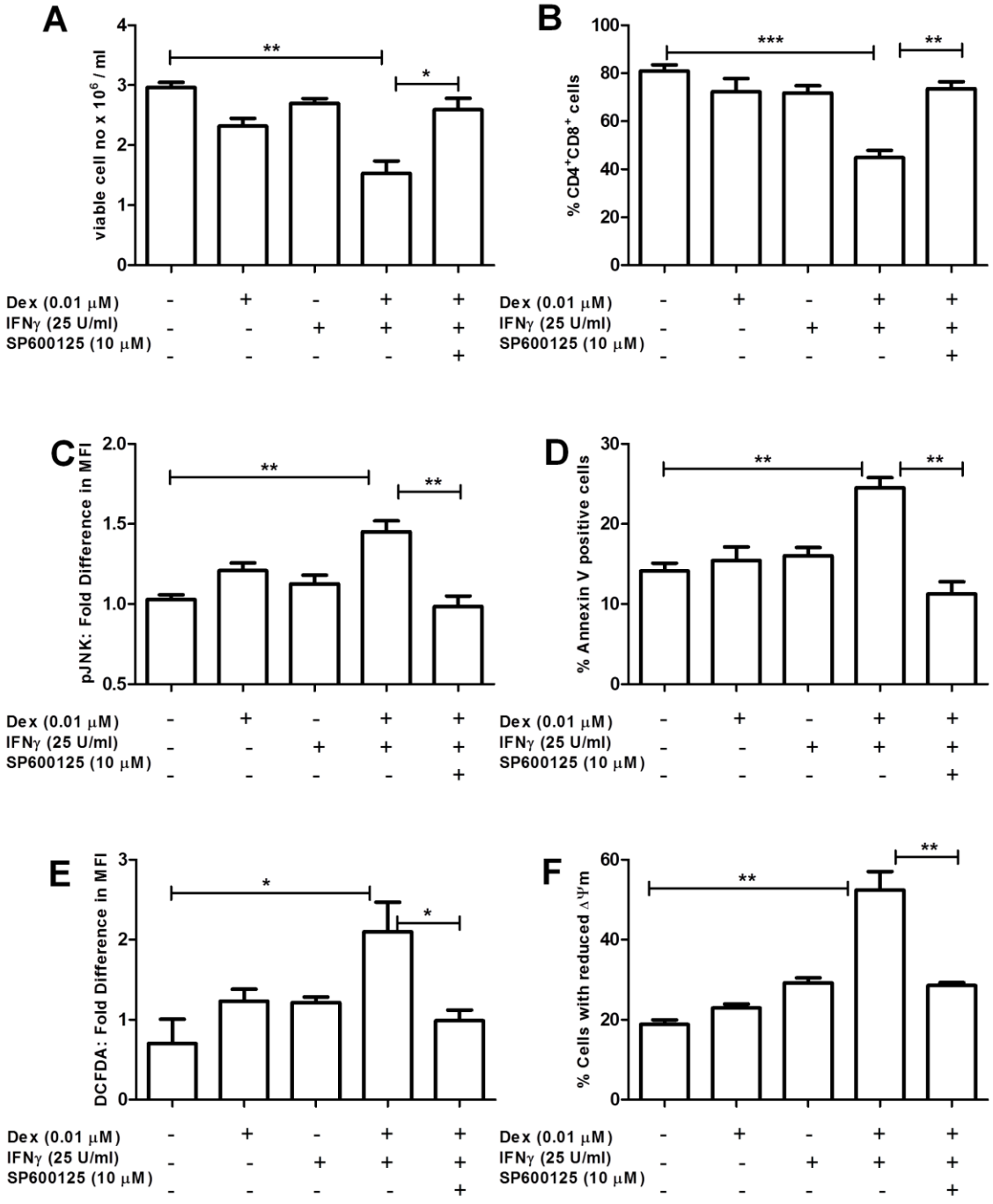

Figure 4. Inhibition of JNK signaling rescues *S. typhimurium* infection-induced thymic atrophy. C57BL/6 mice were infected (*Stm*) with 10^8 CFU *S. typhimurium* and treated with 25 mg/kg SP600125 (*Stm* + SP600125), unless otherwise indicated. (A, B) CFU and (C, D) viable cell numbers were determined on day 4 post infection. (E) Survival analysis of infected and SP600125 treated mice was performed. (F) The number of viable thymocytes in different subsets control (UI), infected and SP600125 treated mice were estimated. (A-F) Data are shown as mean ± SEM of 5 mice per group from one experiment representative of four independent experiments performed. (G) Histological analysis of thymi from the indicated groups was performed by staining with hematoxylin and eosin. Images were obtained at 100x magnification using a light microscope fitted with Nikon camera. * $p \leq 0.05$, ** $p \leq 0.01$ and *** $p \leq 0.001$, Student's *t* test.

Figure 4

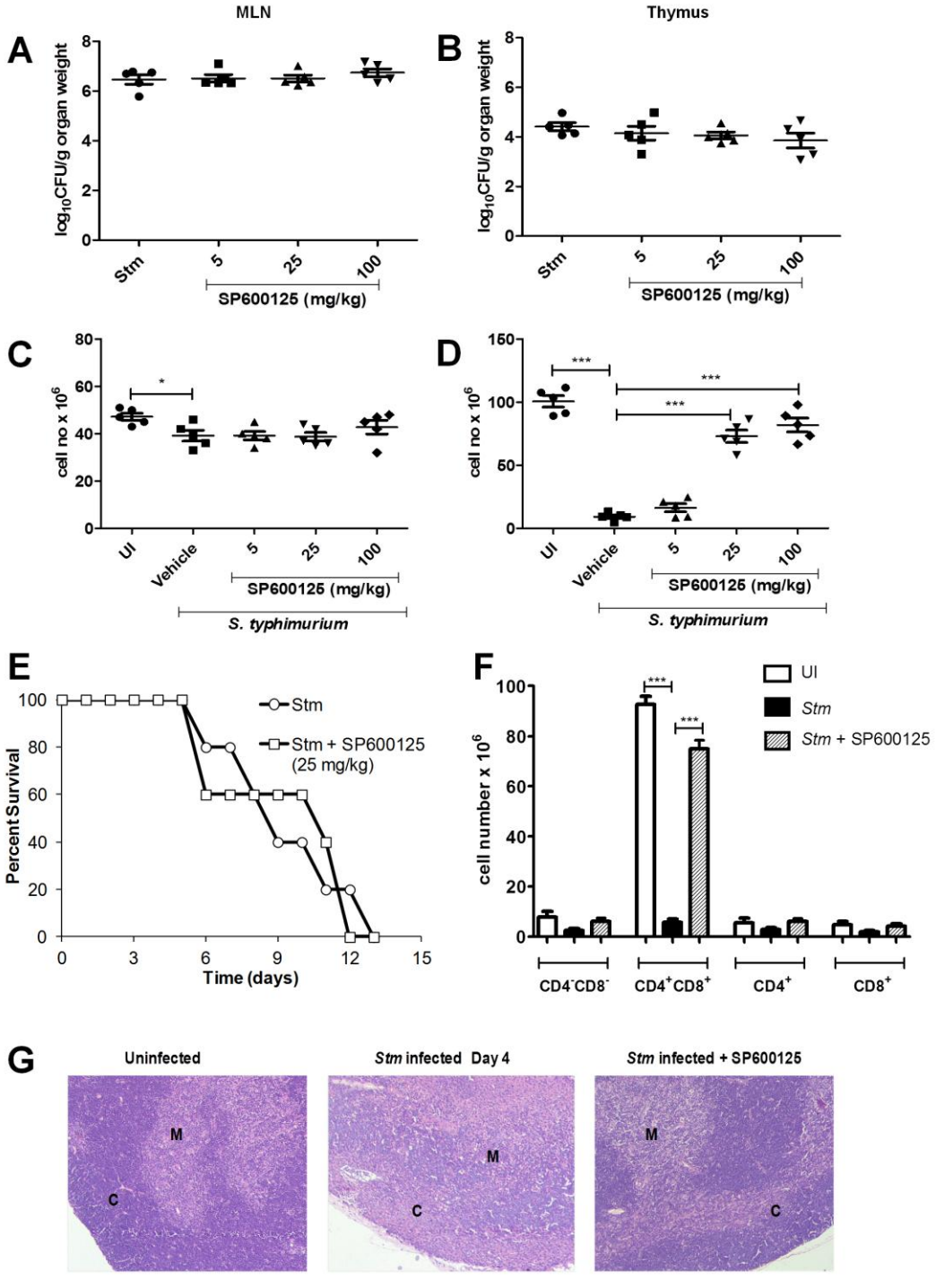

Figure 5. JNK activation upon *S. typhimurium* infection elicits apoptotic death processes. Thymocytes were isolated from control (UI), infected (*Stm*) and infected with 25 mg/kg SP600125 treated (*Stm* + SP600125) C57BL/6 mice. (A) Intracellular ROS, (B) Annexin V and PI staining, (C) mitochondrial potential and (D) caspase 3 activity in thymocyte populations from indicated groups were determined. (E, F) The fold difference in intracellular amounts of (E) Bax and (F) Bcl-xL in thymocyte subsets was determined. The data are shown as mean + SEM of 5-7 mice per group pooled from three independent experiments. * $p \leq 0.05$, ** $p \leq 0.01$ and *** $p \leq 0.001$, Student's *t* test.

Figure 5

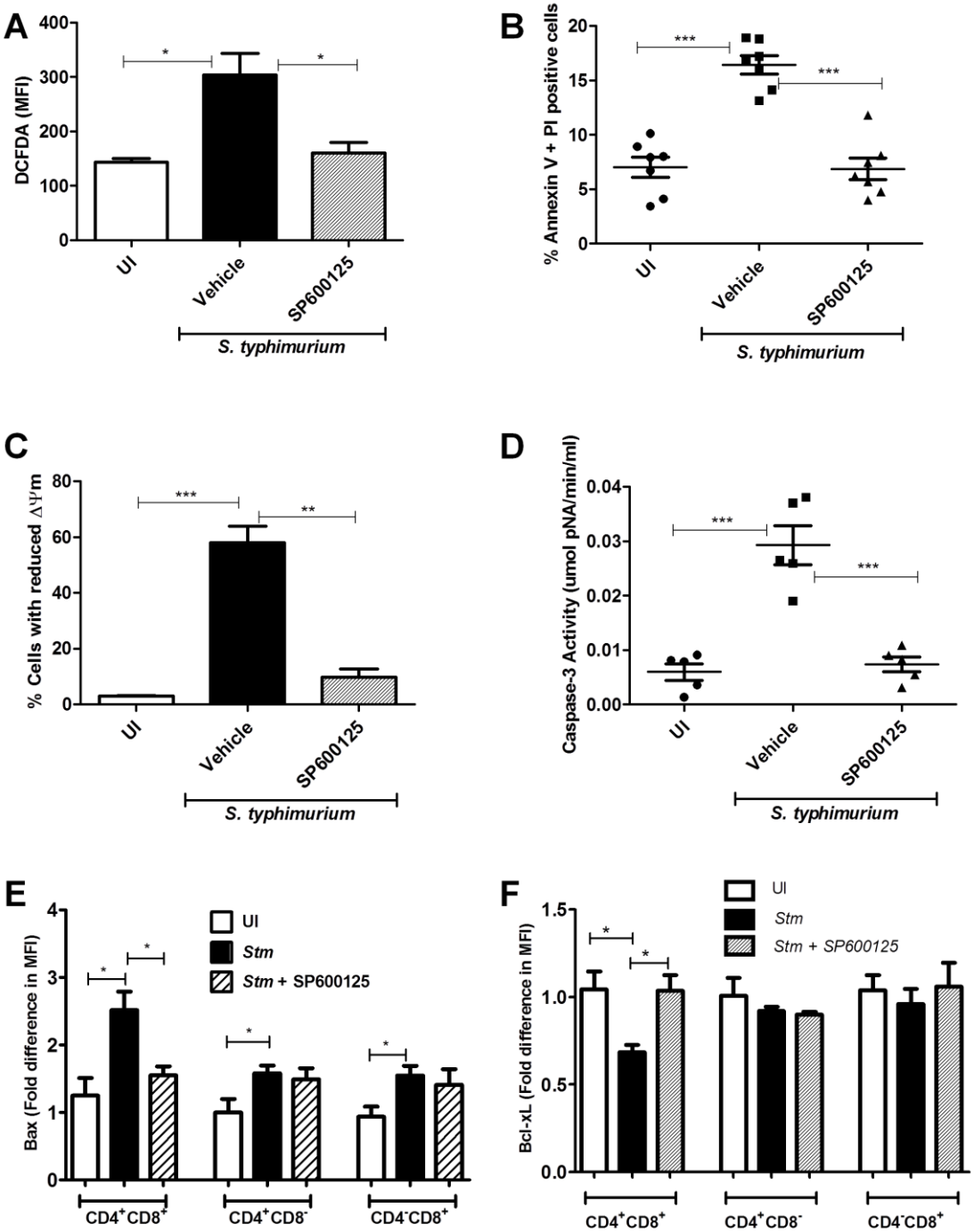

Figure 6. JNK activation enhances in vivo amounts of cortisol and inflammatory cytokines during *S. typhimurium* infection. Serum samples were collected on day 4 post infection from uninfected (UI) and infected C57BL/6 mice in the absence (*Stm*) or presence (*Stm* + SP600125) of SP600125 (25 mg/kg) treatment. Serum amounts of (A) Cortisol, (B) TNF-α, (C) IFN-γ, (D) IL-1β and (E) IL-6 were quantified using ELISA. Each symbol represents an individual mouse and bars represent mean + SEM. Data shown are pooled from three independent experiments. * $p \leq 0.05$, ** $p \leq 0.01$ and *** $p \leq 0.001$, Student's *t* test.

Figure 6